

## Discovery and Structure–Activity Relationship of Oxalylarylaminobenzoic Acids as Inhibitors of Protein Tyrosine Phosphatase 1B

Gang Liu,<sup>\*,†</sup> Bruce G. Szczepankiewicz,<sup>†</sup> Zhonghua Pei,<sup>†</sup> David A. Janowick,<sup>†,§</sup> Zhili Xin,<sup>†</sup> Philip J. Hajduk,<sup>‡</sup> Cele Abad-Zapatero,<sup>‡</sup> Heng Liang,<sup>‡</sup> Charles W. Hutchins,<sup>‡</sup> Stephen W. Fesik,<sup>‡</sup> Steve J. Ballaron,<sup>†</sup> Mike A. Stashko,<sup>†</sup> Tom Lubben,<sup>†</sup> Amanda K. Mika,<sup>†</sup> Bradley A. Zinker,<sup>†</sup> James M. Trevillyan,<sup>†</sup> and Michael R. Jirousek<sup>†,§</sup>

Metabolic Disease Research and Advanced Technology, Global Pharmaceutical Research and Development, Abbott Laboratories, Abbott Park, Illinois 60064-6098

Received December 18, 2002

Protein Tyrosine phosphatase 1B (PTP1B) has been implicated as a key negative regulator of both insulin and leptin signaling pathways. Using an NMR-based screening approach with <sup>15</sup>N- and <sup>13</sup>C-labeled PTP1B, we have identified 2,3-dimethylphenyloxalylaminobenzoic acid (**1**) as a general, reversible, and competitive PTPase inhibitor. Structure-based approach guided by X-ray crystallography facilitated the development of **1** into a novel series of potent and selective PTP1B inhibitors occupying both the catalytic site and a portion of the noncatalytic, second phosphotyrosine binding site. Interestingly, oral bioavailability has been observed in rats for some compounds. Furthermore, we demonstrated in vivo plasma glucose lowering effects with compound **12d** in ob/ob mice.

### Introduction

Type II diabetes is a progressive disease of metabolic dysregulation characterized by insulin resistance in peripheral tissues (liver, muscle, and adipose) and impaired insulin secretion by the pancreas. At the molecular level, the mechanism of insulin resistance in type II diabetes appears to involve defects in postreceptor signal transduction<sup>1,2</sup> and is not due to a structural defect in the insulin receptor (IR) itself.<sup>3</sup> Initial binding of insulin to the IR evokes a cascade of phosphorylation events, including the autophosphorylation of the IR on multiple tyrosine residues,<sup>4</sup> tyrosine phosphorylation of IR substrate (IRS) proteins (IRS-1 to -4) and other adaptor molecules.<sup>5</sup> Eventually, the metabolic effect of insulin signaling is manifested with the uptake of glucose into the peripheral tissues.<sup>6</sup>

The activation of the IR by autophosphorylation is reversed by the action of protein tyrosine phosphatases (PTPases). To date, biochemical, “substrate-trapping”, and in vivo studies favor PTPase 1B (PTP1B) as the protein phosphatase directly dephosphorylating the IR.<sup>7</sup> The most compelling data came from the targeted disruption of the PTP1B gene in mice.<sup>8,9</sup> Two laboratories have independently generated PTP1B knockout mice. These mice exhibit increased insulin sensitivity and improved glucose tolerance. Unexpectedly, PTP1B deficiency in these mice provided a protective effect on diet-induced obesity, enhanced response toward leptin-mediated weight loss, and suppression of feeding. Subsequently, substrate-trapping experiments demonstrate that leptin-activated Janus kinase 2 (Jak2) is a

substrate of PTP1B.<sup>10,11</sup> The evidence strongly suggests that selective small-molecule inhibitors of PTP1B may be effective therapeutics in treating insulin resistance, type II diabetes, and obesity.

Recent studies have provided important insight into the basic structural requirements for PTP1B–substrate and –inhibitor interactions and have suggested that identification of highly selective, catalytic site-directed PTP1B inhibitors are quite possible.<sup>12</sup> However, despite the significant progress made toward developing PTP1B inhibitors, most of the specific inhibitors reported to date do not possess oral bioavailability for potential clinical use. In this communication, we now describe the discovery of 2,3-dimethylphenyloxalylaminobenzoic acid (**1**) as a novel general PTPase inhibitor scaffold through an NMR-based screening. A detailed structure–activity relationship (SAR) and the development of this series of compounds into potent, selective, orally available inhibitors of PTP1B with in vivo efficacy in ob/ob mice are also reported.

### Chemistry

Analogues varying the 2,3-dimethylaniline portion of **1** were prepared via two different routes. In method A (Scheme 1), a Buchwald coupling between the *o*-bromocinnamate **2** and naphthylamine **3**, followed by the oxidative cleavage of the resulting quinolone **4** provided the final product **5**.<sup>13</sup> A more general route (method B) started with a condensation between diphenyliodonium carboxylate (DPIC) and the appropriate aniline (Scheme 2).<sup>14</sup> The sterically hindered *sec*-aniline **6** could be acylated with ethyloxalyl chloride through an intramolecular acyl-transfer reaction. Subsequent saponification of the monoester **7** provided the desired oxamic acid **8**.

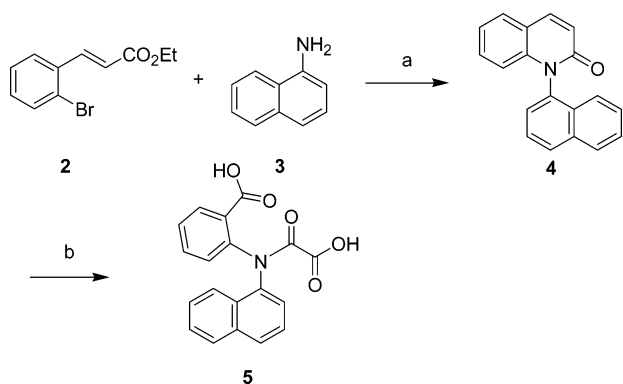
Scheme 3 described the synthesis of requisite *p*-aminophenylalanine derivatives for condensation with DPIC. Heck coupling of 4-bromoaniline derivatives with methyl 2-acetamidoacrylate yielded the dehydroamino

\* To whom correspondence should be addressed. Address: Metabolic Disease Research, R4MC, AP-10, Abbott Laboratories, 100 Abbott Park Road, Abbott Park, IL 60064-6098. Phone: 847-935-1224. Fax: 847-938-1674. E-mail: gang.liu@abbott.com.

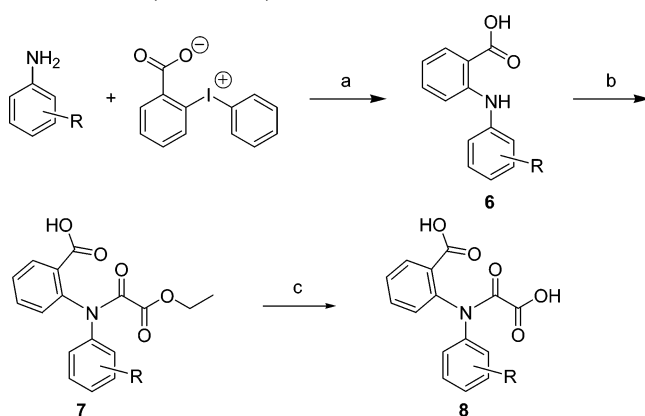
<sup>†</sup> Metabolic Disease Research.

<sup>§</sup> Current Address: Pfizer Global R&D, La Jolla Laboratories, 10770 Science Center Drive, San Diego, CA 92121-1187.

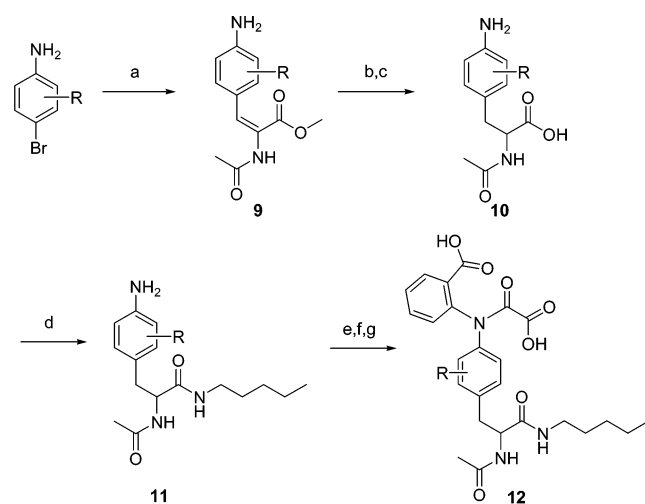
<sup>‡</sup> Advanced Technology.

**Scheme 1.** (Method A)<sup>a</sup>

<sup>a</sup> Reagents and conditions: (a) Pd<sub>2</sub>(dba)<sub>3</sub>, 2-dicyclohexylphosphanyl-2'-dimethylaminobiphenyl, 60% NaH, toluene, 110 °C; (b) KMnO<sub>4</sub>, Pyr/H<sub>2</sub>O, room temp.

**Scheme 2.** (Method B)<sup>a</sup>

<sup>a</sup> Reagents and conditions: (a) Cu(OAc)<sub>2</sub>, *i*-PrOH, 85 °C; (b) ClCOCO<sub>2</sub>Et, *i*-Pr<sub>2</sub>NEt, CH<sub>2</sub>Cl<sub>2</sub>, 0 °C to room temp; (c) NaOH, MeOH, room temp.

**Scheme 3**<sup>a</sup>

<sup>a</sup> Reagents and conditions: (a) methyl acetamidocrylate, Pd(OAc)<sub>2</sub>, P(*o*-tolyl)<sub>3</sub>, Et<sub>3</sub>N, DMF, 110 °C; (b) 10% Pd/C, MeOH/EtOAc, atm of H<sub>2</sub>, 50 °C; (c) NaOH, MeOH, room temp; (d) EDCI, HOBT, amyl amine, Et<sub>3</sub>N, DMF; (e) DPIC, Cu(OAc)<sub>2</sub>, DMF, 95 °C; (f) ClCOCO<sub>2</sub>Et, *i*-Pr<sub>2</sub>NEt, CH<sub>2</sub>Cl<sub>2</sub>, 0 °C to room temp; (g) NaOH, MeOH, room temp.

ester **9**. The double bond of **9** was hydrogenated to give the *p*-aminophenylalanine methyl ester, which was then hydrolyzed to give the acid **10**. Coupling of **10** with amylamine yielded the diamide **11**, which was then

converted to the desired oxamic acid **12** following condensation with DPIC, acylation, and hydrolysis.

The enantiomerically pure analogue **17** was synthesized from the readily available aniline **13** (Scheme 4). Monoiodination of **13** with in situ generated ICl provided the iodide **14**. The aniline **15** derived from DPIC condensation with **14** was then coupled with acrylamide to generate the diarylaniline **16**. The standard acylation and hydrolysis protocol yielded **17**.

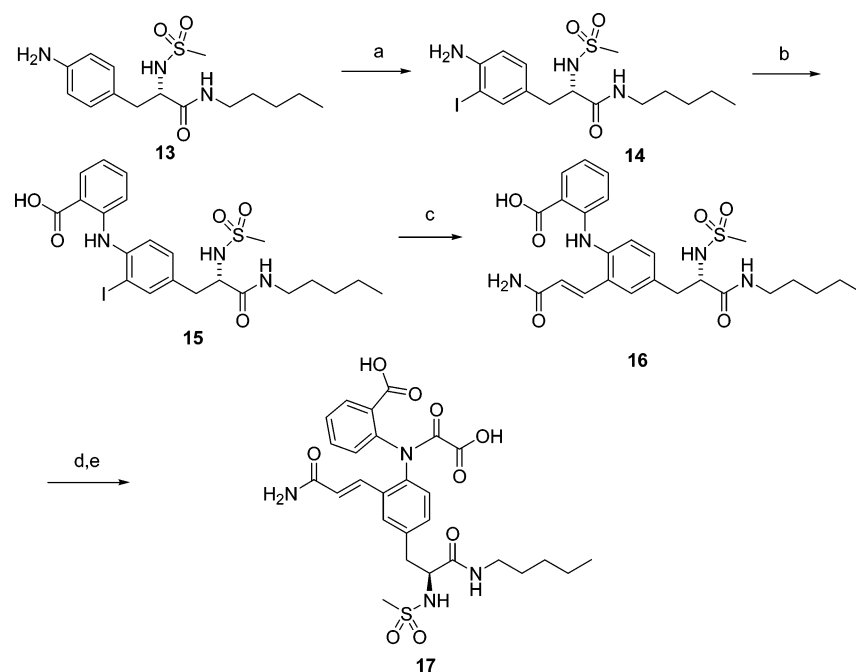
**Results and Discussion**

**NMR Screening.** To identify small molecule novel phosphotyrosine (pTyr) mimetics that could serve as inhibitors of PTP1B, an NMR-based screen was employed.<sup>15,16</sup> With uniformly <sup>15</sup>N-labeled PTP1B (residues 1–288), more than 10 000 low molecular weight compounds (MW ≤ 350 Da) were tested for binding to this enzyme. From this screen, 2,3-dimethylphenyloxalylaminobenzoic acid (**1**) was identified as an active site binder as evidenced by chemical shift perturbations for the amide resonances of Val49, Gly220, and Gly218 residues in the catalytic site (see Figure 1). NMR titrations yielded an estimated *K<sub>d</sub>* value of 100 μM for **1** (Table 1).

A detailed kinetic analysis of **1** was then conducted using *p*NPP as the small-molecule substrate in a continuously monitored colorimetry assay. Compound **1** exhibited classical kinetic behavior for a competitive, reversible inhibitor with an inhibition constant (*K<sub>i</sub>*) of 93 μM, consistent with the affinity measured by NMR (Table 1). Unlike the character displayed by a previously reported series of PTP1B inhibitors,<sup>17</sup> the *K<sub>i</sub>* value of **1** does not depend on the pH of the assay buffer system. Kinetic analysis of **1** against other PTPases in a selectivity panel indicated that **1** was a general phosphatase inhibitor with very little discrimination among PTP1B, T-cell PTPase (TCPTP), leukocyte antigen-related tyrosine phosphatase (LAR), CD45, and SH2-domain-containing phosphotyrosine phosphatase-2 (SHP-2). Therefore, oxalylarylaminobenzoic acid based compounds, such as **1**, represent a novel series of pTyr mimetics.

In an effort to increase the potency of **1**, analogues varying the 2,3-dimethylaniline were prepared. These new analogues were then evaluated for their ability to inhibit PTP1B in both the NMR titration and colorimetry assay. To provide higher sensitivity and more accurate *K<sub>d</sub>* determination, selectively <sup>13</sup>C-labeled PTP1B was used for the NMR studies on these analogues.<sup>18</sup> In general, data from both NMR titration and colorimetry assay agreed with each other very well. As shown in Table 1, both regioisomers of the naphthalenylamine-derived analogues **5** and **8a** showed 3- to 4-fold improvement over **1**. More importantly, 7-hydroxynaphthalen-1-ylamine-derived **8b** showed further improvement of affinity, according to both the NMR titration and *K<sub>i</sub>* analysis. The tetrahydronaphthalene analogue **8c** was only slightly better than **1**, underlying the importance of the aromaticity of the naphthalene ring.

**X-ray Crystallography.** The improved potency of analogues such as **5** and **8b** facilitated the determination of their binding modes using X-ray crystallography. Diffraction (resolution of 2.2 Å) of the PTP1B crystal (1–322) soaked with **8b** revealed an unusual binding mode of this series of pTyr mimetics.<sup>19</sup>

Scheme 4<sup>a</sup>

<sup>a</sup> Reagents and conditions: (a) NaI, chloramine-T, AcOH, room temp; (b) DPIC, Cu(OAc)<sub>2</sub>, DMF, 95 °C; (c) acrylamide, Pd(OAc)<sub>2</sub>, Pd(OAc)<sub>2</sub>, Et<sub>3</sub>N, DMF, 110 °C; (d) ClCOCO<sub>2</sub>Et, *i*-Pr<sub>2</sub>NEt, CH<sub>2</sub>Cl<sub>2</sub>, 0 °C to room temp; (e) NaOH, MeOH, room temp.

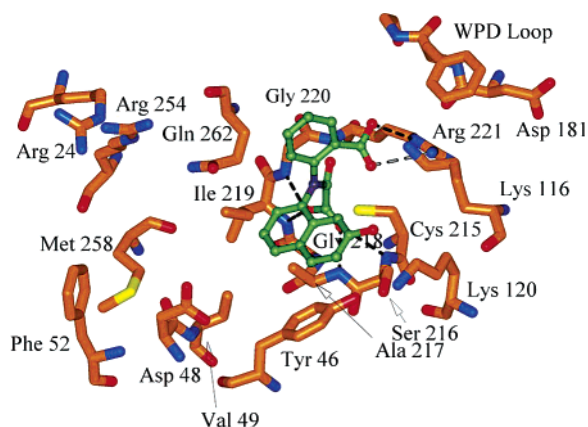


**Figure 1.** X-ray crystal structure (2.2 Å) of PTP1B soaked with compound **8b**. Carbon is in orange and green for compound **8b**, oxygen is in red, nitrogen is in blue, and sulfur is in yellow. Selected hydrogen bonds are indicated by dashed lines.

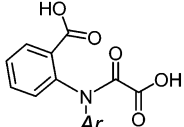
All PTPases have a highly conserved catalytic pocket with the “signature motif” (I/V)HCX<sub>3</sub>R(S/T)G, which forms a semicircular cage around the pTyr phosphate. Binding of phosphotyrosine into the catalytic pocket of PTP1B causes a conformational change in the enzyme, bringing a flexible WPD (tryptophan, proline, aspartic acid) loop containing Asp181 into proximity with the phosphotyrosine substrate. Formation of the thiolphosphoryl enzyme intermediate is facilitated by Asp181, which acts as a general acid by providing a proton to the leaving phenolic group and as a general base by accepting a proton from water during the hydrolysis of the thiolphosphoryl enzyme intermediate.

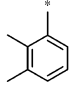
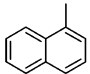
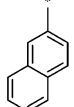
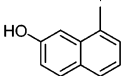
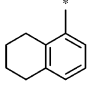
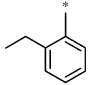
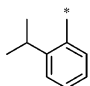
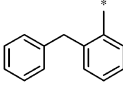
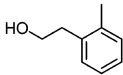
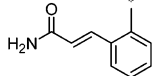
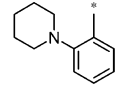
The most unusual feature revealed by the X-ray crystal structure of the PTP1B/**8b** complex is the conformation of the WPD loop (Figure 1). With **8b** bound to PTP1B, the flexible loop is in its native, presubstrate binding conformation, i.e., the open conformation. The

benzoic acid of **8b** acts as the physical barrier that prevents the WPD loop from adopting the closed conformation. A unique hydrogen-bonding network is formed in the catalytic site involving Arg221, Gly220, Ile219, Ala217, and Ser216. The hydroxy group of the naphthalene resides in a hydrophilic pocket formed largely by the hydroxy groups of Tyr46 and Ser216 and the amino groups of Lys116 and Lys120. van der Waals interaction is observed between the side chain of Gln262 and the aromatic portion of the benzoic acid. A  $\pi$ - $\pi$  interaction is also noted between the naphthalene ring and Tyr46. The open conformation of the WPD loop exposes additional hydrophobic residues, such as the hydrophobic portions of Lys116, Lys120, and Asp181 in the catalytic site, which have not been available to the inhibitors bound to PTP1B with the WPD loop in the closed conformation.<sup>20</sup>

**SAR Development.** On the basis of the binding space revealed by the X-ray structure of **8b**, the ortho substituents of the aryl group of **1** were further explored. *o*-Ethyl- (**8d**), *o*-isopropyl- (**8e**), and *o*-benzyl- (**8f**) aniline-based analogues showed 2- to 4-fold improvement in binding affinity compared to **1**. Further potency improvement was observed with the *o*-hydroxyethyl analogue (**8g**,  $K_i = 17 \mu\text{M}$ ), which was designed to mimic the binding of the 7-hydroxynaphthalene analogue **8b**. Further expansion of the hydrogen-bonding interaction of the hydroxy group of **8g** led to the synthesis of acrylamide-based **8h** with slightly improved inhibitory potency. Interestingly, an *o*-piperidine substituent yielded an inhibitor **8i** with a  $K_i$  value of 14  $\mu\text{M}$ . These results suggested a rather tolerant catalytic binding site for both lipophilic and hydrophilic groups and opportunities for further optimization of the binding elements in the active site.

An analysis of the binding surface near the catalytic site of PTP1B revealed at least three binding pockets: the catalytic site pTyr pocket, the second pTyr site, and

**Table 1.** SAR of the Catalytic Site-Directed Oxalylarylaminobenzoic Acids


compd	Ar	Dissociation Constant ( $K_d$ ) ( $\mu\text{M}$ )	Inhibition Constant ( $K_i \pm \text{SEM}$ ) ( $\mu\text{M}$ )
1		124 ( $100^a$ )	93
5		26	24
8a		11	39
8b		8	$17 \pm 7$
8c		71	74
8d		<50	$60 \pm 16$
8e		49	35
8f		35	$24 \pm 1$
8g		35	$17 \pm 4$
8h		ND	$11 \pm 2$
8i		13	$14 \pm 1$

<sup>a</sup>  $K_d$  derived from  $^{15}\text{N}$ -labeled PTP1B.

the hexapeptide binding site.<sup>21</sup> Zhang and co-workers had identified the noncatalytic, cleftlike phosphotyrosine binding site (site 2) adjacent to the catalytic pocket, which is not conserved among all PTPases and may participate in substrate recognition.<sup>22</sup> The X-ray crystal structure of the insulin receptor peptide, D-pY-pY-R, bound to PTP1B shows the N-terminal phosphotyrosine bound in the catalytic pocket while the C-terminal phosphotyrosine is bound in the second arylphosphate binding site.<sup>23</sup> Our strategy for achieving high

specificity for PTP1B over other closely related phosphatases is through interaction with the active site as well as the neighboring, less homologous site 2.

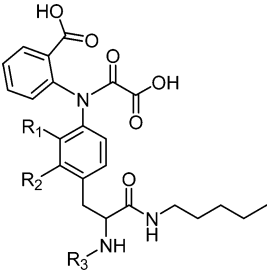
A linker was then sought to branch out of the catalytic site and reach into site 2 with the current template. Since a number of PTP1B inhibitors have utilized an alanine moiety as binding elements beyond the catalytic site pTyr mimetic,<sup>24</sup> an alanine-based linker appeared attractive for initial exploration. The X-ray structure of **8b** suggests that the alanine-based chain could extend out of the active site from the 4-position of the naphthalene, which would also give a system that resembled a natural phosphotyrosine substrate. We therefore prepared a prototype compound **18** according to the route outlined in Scheme 2. The C-terminal pentylamide of **18** was chosen by balancing the hydrophobicity and chain length for reaching site 2. Compound **18** not only exhibited reasonable binding affinity to PTP1B and TCPTP (Table 2), but also established binding to both the catalytic site and part of site 2 simultaneously, according to the X-ray crystal structure (data not shown; see Figure 2 for general binding mode). X-ray structure of **18** also revealed two hydrogen-bonding interactions with Asp48 of PTP1B that are critical for the enhanced affinity. These interactions also position the pentyl group in site 2 of PTP1B, which allows introduction of site 2 ligands with this template. Since the *tert*-butyl carbamate of **18** interacts with Asp48 of PTP1B, a basic amino group in the same position was expected to provide higher binding affinity. Surprisingly, compound **19** was completely inactive against PTP1B and TCPTP. The exact cause for such a dramatic change of potency is not clear. In contrast, compounds containing neutral groups with hydrogen-bonding donors, such as acetamido (**20**) and sulfonamido (**21**), were slightly more potent than **18**.

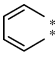
After establishment of a linker for bridging the catalytic site and site 2, an effort toward optimization of this series of compounds was undertaken. As shown in Table 2, naphthyl (**12a**), *o*-ethyl (**12b**), *o*-isopropyl (**12c**), *o*-hydroxyethyl (**12d**), and *o*-piperidinyl (**12e**) based analogues all displayed  $K_i$  values of  $\sim 1 \mu\text{M}$ , with a 10-fold improvement in binding affinity toward PTP1B and TCPTP when compared to **18**. The enantiomerically pure analogue **17** exhibited a submicromolar inhibitory constant ( $K_i = 0.17 \mu\text{M}$ ) for both PTP1B and TCPTP, an over-50-fold improvement over **21**.

The X-ray crystal structure of the PTP1B/**17** complex (resolution of 2.2 Å) as shown in Figure 2 illustrated our structure-based inhibitor design approach.<sup>19</sup> The interactions established between PTP1B and the two carboxylic acids of **8b** remained largely intact for **17** in the catalytic site. Additionally, the acrylamide of **17** was in hydrogen bond contact with the amino group of Lys120 (3.04 Å) and with the benzoic acid (3.09 Å) intramolecularly. As indicated with **18**, two critical hydrogen bonds are observed between **17** and Asp48, with the distance being 2.57 (main chain NH) and 2.44 Å (sulfonamido NH), respectively. The terminus of the pentylamide located in the center of site 2 and is well positioned for further functionalization.

Asp48 has been demonstrated to be a residue for addressing selectivity because of the point mutation between PTP1B/TCPTP and other phosphatases such



**Table 2.** SAR of Oxalylarylaminobenzoic Acids Occupying Both the Catalytic Site and a Portion of Site 2


compd	R <sub>1</sub>	R <sub>2</sub>	R <sub>3</sub>	K <sub>i</sub> ± SEM (μM) PTP1B	K <sub>i</sub> ± SEM (μM) (TCPTP)
<b>18<sup>a</sup></b>	H	H	<i>t</i> -BuOCO-	17.3 ± 1.9	13.0
<b>19<sup>a</sup></b>	H	H	H	>100	>100
<b>20<sup>a</sup></b>	H	H	CH <sub>3</sub> CO-	9.8 ± 2.1	10.9
<b>21<sup>a</sup></b>	H	H	CH <sub>3</sub> SO <sub>2</sub> -	9.1	ND
<b>12a<sup>b</sup></b>		H	CH <sub>3</sub> CO-	1.1 ± 0.5	1.1 ± 0.9
<b>12b<sup>b</sup></b>	-CH <sub>2</sub> CH <sub>3</sub>	H	CH <sub>3</sub> CO-	1.2 ± 0.3	0.9 ± 0.1
<b>12c<sup>b</sup></b>	-CH(CH <sub>3</sub> ) <sub>2</sub>	H	CH <sub>3</sub> CO-	1.2 ± 0.1	1.2 ± 0.3
<b>12d<sup>b</sup></b>	-CH <sub>2</sub> CH <sub>2</sub> OH	H	CH <sub>3</sub> CO-	1.5 ± 0.7	1.5 ± 0.6
<b>12e<sup>b</sup></b>	1-piperidinyll	H	CH <sub>3</sub> CO-	2.0 ± 1.5	ND
<b>17<sup>a</sup></b>	-( <i>E</i> )CH <sub>2</sub> =CH <sub>2</sub> CONH <sub>2</sub>	H	CH <sub>3</sub> SO <sub>2</sub> -	0.17 ± 0.07	0.16 ± 0.06

<sup>a</sup> (S)-Enantiomer. <sup>b</sup> 1:1 racemic mixture.

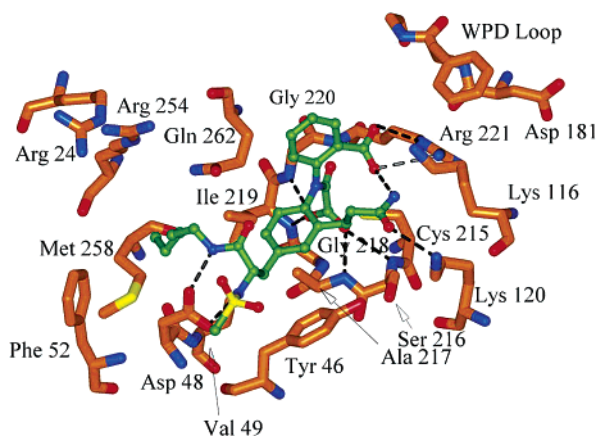


**Figure 2.** X-ray crystal structure (2.2 Å) of PTP1B soaked with compound **17**. Carbon is in orange and green for compound **17**, oxygen is in red, nitrogen is in blue, and sulfur is in yellow. Selected hydrogen bonds are indicated by dashed lines.

as LAR (Asn48) and SHP-2 (Asn48).<sup>17</sup> Therefore, we were gratified to find that compound **12a** is selective for PTP1B and TCPTP over other PTPases. As shown in Table 3, compound **12a** showed 6-, 30-, and greater than 300-fold selectivity for PTP1B/TCPTP over LAR, SHP-2, and CD45, respectively. Additionally, **12a** also exhibited excellent selectivity profiles over a dual specificity phosphatase cdc25 (>300-fold) and a protein serine/threonine phosphatase calcineurin (>300-fold). TCPTP has the highest homology to PTP1B, with 74% sequence identity in the catalytic domain, the catalytic site being identical. Therefore, it is not surprising to note that compound **12a** and its closely related analogues inhibited PTP1B and TCPTP equally well. PTP1B inhibitors, such as **12a**, are well positioned for further exploring the less homologous site 2 for achieving selectivity over TCPTP.

**In Vivo Studies.** Despite the fact that these dicarboxylic acid containing PTP1B inhibitors have low cellular permeability in a Caco-2 permeability study

(data not shown), some of them have been found to be orally bioavailable in Sprague–Dawley rats. Following a 5 mg/kg (mpk) oral dose, the nonselective inhibitor **5** achieved a high AUC (30.6 μg·h/mL) and long half-life (7.3 h) and had a bioavailability value of 17% (Table 4). For the more selective analogues, such as **12b** and **12d**, oral AUC (0.94 and 0.55 μg·h/mL, respectively) decreased and the volume of distribution (3.6 and 18.6 L/kg, respectively) increased dramatically following a 5 mpk dose, indicating a possible accumulation in the peripheral tissues. Since PTP1B is an intracellular protein target, the possible accumulation in insulin-responsive tissues would be a desirable attribute for small-molecule inhibitors. Bioavailability values of 23% and 17% were calculated for **12b** and **12d**, respectively.

Compound **12d** was then evaluated in vivo for its ability to lower plasma glucose and insulin levels in the genetically obese C57 BL/6J ob/ob diabetic mouse model. To maximize compound exposure, **12d** was given subcutaneously via minipump to ob/ob mice at 30 and 120 mpk for 6 days. After 6 days of continuous infusion, the plasma glucose levels of ob/ob mice from the **12d**-treated groups decreased dose-dependently when days 1 and 6 are compared. The plasma glucose level of the rosiglitazone-treated group (a positive control) reached the level of lean control animals.

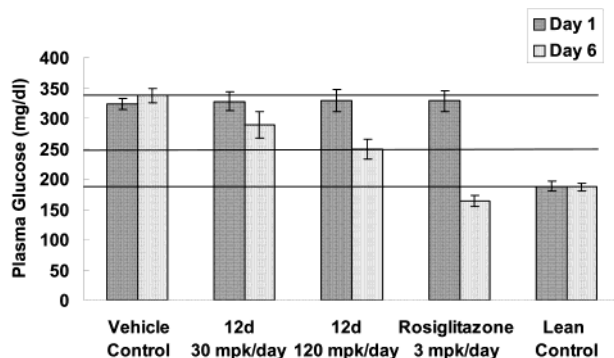
Figure 3 shows the reduction of the plasma glucose level in ob/ob mice from this study. We observed an average of 12% and 24% reduction of plasma glucose levels with 30 and 120 mpk/day treatment of **12d**, respectively, and 50% reduction with 3 mpk/day treatment of rosiglitazone. However, results from the plasma insulin levels were less clear. For the 30 mpk treatment group, we observed a reduction of insulin level (from 35 ng/mL for the vehicle control group to 22 ng/mL), which was consistent with the reduction of plasma glucose level and increased insulin sensitivity. For the 120 mpk treatment group, the insulin level actually remained about the same (37 ng/mL) as the vehicle control. The rosiglitazone treatment group showed

**Table 3.** Phosphatase Selectivity Profile of Compound **12a**

compd	$K_i \pm \text{SEM}$ ( $\mu\text{M}$ )						
	PTP1B	TCPTP	LAR	SHP-2	CD45	cdc25	calcineurin
<b>12a</b>	1.1 $\pm$ 0.5	1.1 $\pm$ 0.9	6.7 $\pm$ 4.7	29.6 $\pm$ 3.6	>300	>300	>300

**Table 4.** Pharmacokinetic Profiles of Selected PTP1B Inhibitors Following Five mpk Doses in Rats

compd	CLp (iv) (L/(h·kg))	V $\beta$ (L/kg)	$t_{1/2}$ (oral) (h)	$C_{\text{max}}$ (oral) ( $\mu\text{g}/\text{mL}$ )	AUC (oral) ( $\mu\text{g}\cdot\text{hr}/\text{mL}$ )	F (%)
<b>5</b>	0.03	0.29	7.3	1.72	30.6	16.8
<b>12b</b>	1.21	3.59	1.2	0.69	0.94	22.6
<b>12d</b>	1.53	18.6	9.0	0.09	0.55	16.7

**Figure 3.** Plasma glucose lowering effects of **12d** following a 6-day treatment in ob/ob mice.

substantial reduction of plasma insulin level as expected (6 versus 2 ng/mL for the lean control). Also, it is important to note that the same degree of body weight increase was seen across the compound-treated groups and the control groups following the 6-day study (data not shown). So we were cautiously encouraged by the initial in vivo results with **12d**, which seemed to support further optimization of this series of compounds.

In conclusion, a novel oxalylarylamino benzoic acid based pTyr mimetic was discovered through an NMR-based fragment screening, and the unique binding mode of this series of inhibitors to PTP1B was determined by X-ray crystallography. The structure-based approach facilitated the development of this series of potent and selective PTP1B inhibitors, which occupy both the catalytic site and part of the less homologous, second phosphotyrosine binding site. Although the core structure of these inhibitors is charged, we have observed reasonable bioavailability in rats for some compounds and demonstrated plasma glucose lowering effects with compound **12d** in ob/ob mice. These inhibitors set the stage for screening novel site 2 ligands and achieving selectivity against the most homologous phosphatase, TCPTP, which will be reported in due course.

## Experimental Section

**General.** Unless otherwise specified, all solvents and reagents were obtained from commercial suppliers and used without further purification. All reactions were performed under nitrogen atmosphere unless specifically noted. Flash chromatography was performed using silica gel (230–400 mesh) from E. M. Science. Proton NMR spectra were recorded on a Varian Mercury 300 NMR spectrometer or a Varian UNITY 400/500, as specified for individual compounds. NMR spectral experiments were run with Me<sub>4</sub>Si as an internal standard, and spectra are reported as shift (multiplicity, coupling constants, proton counts). Mass spectral analyses

were accomplished on a Finnigan SSQ7000 GC/MS mass spectrometer using electrospray ionization (ESI) technique. Exact mass measurements were performed on a Finnigan FTMS Newstar T70 mass spectrometer. The compound is determined to be “consistent” with the chemical formula if the exact mass measurement is within 5.0 ppm relative mass error (RME) of the exact monoisotopic mass. The purity of the compounds was determined on two analytic HPLC systems to be of greater than 90% purity.

Preparative HPLC was performed on an automated Gilson HPLC system, using a SymmetryPrep Shield RP18 prep cartridge, 25 mm  $\times$  100 mm i.d., S-7  $\mu\text{M}$ , and a flow rate of 25 mL/min;  $\lambda$  = 214, 245 nm; mobile phase A, 0.1% TFA in H<sub>2</sub>O; mobile phase B, CH<sub>3</sub>CN; linear gradient 0–70% of B in 19 min. The purified fractions were evaporated to dryness on a Savant SpeedVac. Analytical HPLC experiments for selected compounds were performed on two systems. For system A, samples were analyzed by a Gilson analytical HPLC system, using a YMC C-18 column (50 mm  $\times$  4.6 mm i.d., S-5  $\mu\text{M}$ , 120 Å). Solvent system used was acetonitrile/0.1% aqueous TFA, gradient 0–70% over 15 min @ 2 mL/min. System B: Samples were analyzed by HPLC/MS/ELSD on an Open Access Finnigan Navigator/Agilent 1100/Sedere Sedex 75 system using a Phenomenex Luna C8 column (5  $\mu\text{m}$ , 2.1 mm  $\times$  50 mm). The solvent system used was acetonitrile/0.1% aqueous TFA, and the gradient was 10–100% over 4.5 min at 1.5 mL/min. The MS was operated in the +APCI mode.

## General Synthesis of Oxalylarylamino benzoic Acids.

**Method A, Exemplified by Compound 5. 1-Naphthalen-1-yl-1H-quinolin-2-one (4).** A mixture of 3-(2-bromophenyl)acrylic acid methyl ester (**2**, 135 mg, 0.56 mmol), 1-aminonaphthalene (**3**, 80 mg, 0.56 mmol), tris(dibenzylideneacetone)dipalladium(0) (**3** mg, 0.003 mmol), 2-dicyclohexylphosphino-2'-(*N,N*-dimethyl)aminobiphenyl (**4** mg, 0.01 mmol), and 60% NaH dispersion in mineral oil (50 mg, 1.2 mmol) in toluene (2 mL) was heated to reflux for 5.5 h, diluted with water (10 mL) and 1 N HCl (5 mL), and extracted with ethyl acetate. The combined extracts were washed with water and brine, dried (MgSO<sub>4</sub>), filtered, and concentrated. The concentrate was purified by flash column chromatography on silica gel with 1:1 ethyl acetate/hexanes to provide 97 mg (0.36 mmol, 64% yield) of **4**. <sup>1</sup>H NMR (300 MHz, DMSO-*d*<sub>6</sub>)  $\delta$  8.16 (d,  $J$  = 9.5 Hz, 2H), 8.12 (d,  $J$  = 8.1 Hz, 1H), 7.84 (dd,  $J$  = 7.6, 1.5 Hz, 1H), 7.74 (dd,  $J$  = 8.1, 7.1 Hz, 1H), 7.60 (dd,  $J$  = 8.1, 1.0 Hz, 1H), 7.57 (dt,  $J$  = 7.3, 1.4 Hz, 1H), 7.46 (ddd,  $J$  = 8.4, 7.0, 1.3 Hz, 1H), 7.32 (ddd,  $J$  = 8.5, 7.1, 1.4 Hz, 1H), 7.25 (dd,  $J$  = 7.5, 1.4 Hz, 1H), 7.20 (dd,  $J$  = 7.6, 1.0 Hz, 1H), 6.78 (d,  $J$  = 9.5 Hz, 1H), 6.30 (d,  $J$  = 8.5 Hz, 1H); MS (ESI) (M + H)<sup>+</sup> at *m/z* 272.

**2-(Naphthalen-1-yloxy)lamino benzoic Acid (5).** A solution of **4** (97 mg, 0.36 mmol) in 1.2 mL of pyridine at room temperature was treated with 1.2 mL of water, cooled to 0 °C, treated with KMnO<sub>4</sub> (210 mg, 1.3 mmol), warmed to room temperature, and stirred for 17 h. The mixture was treated with methanol (0.2 mL), stirred for 5 min, treated with 1 N NaOH (4 mL), and filtered through diatomaceous earth (Celite). The filter cake was washed with water (15 mL), and the combined filtrates were washed with diethyl ether, cooled to 0 °C, adjusted to less than pH 3 with 12 N HCl, and extracted with ethyl acetate. The combined extracts were washed with brine, dried (MgSO<sub>4</sub>), filtered, and concentrated. The concentrate was purified by reverse-phase HPLC to provide **5** (35 mg, 0.10 mmol, 29% yield) as a 3:2 mixture of rotamers. <sup>1</sup>H NMR (3:2 mixture of rotamers) (500 MHz, DMSO-*d*<sub>6</sub>)  $\delta$  8.37 (d,  $J$  = 8.7 Hz, 1H), 8.05–8.03 (m, 1H), 8.01–7.95 (m, 1H), 7.87 (dd,  $J$  = 1.8, 7.7 Hz, 1H), 7.68–7.73 (m, 1H), 7.63–7.59 (m, 1H), 7.57–7.49 (m, 2H), 7.45–7.38 (m, 1H), 7.34 (dt,  $J$  = 7.5, 1.1 Hz, 1H), 7.21 (d,  $J$  = 7.7 Hz, 1H), 6.89 (d,  $J$  = 7.3 Hz, 1H); MS (ESI) (M + H)<sup>+</sup> at *m/z* 336; HRMS calcd

for (M + H)<sup>+</sup> C<sub>19</sub>H<sub>14</sub>N<sub>1</sub>O<sub>5</sub> 336.0872, found 336.0881; analytical HPLC *t*<sub>R</sub> = 6.05 min (A), *t*<sub>R</sub> = 1.80 min (B).

**General Synthesis of Oxalylarylaminobenzoic Acids. Method B, Exemplified by Compound 1. 2-(2,3-Dimethylphenylamino)benzoic Acid (6; R = 2,3-Dimethyl).** To a mixture of 2,3-dimethylaniline (1.21 g, 10.0 mmol), diphenyliodonium 2-carboxylate monohydrate (3.42 g, 10.0 mmol), and copper(II) acetate (73 mg, 0.40 mmol) was added 40 mL of 2-propanol. The mixture was stirred at reflux under N<sub>2</sub> for 23 h and then concentrated in vacuo. The solid residue was taken up in 100 mL of ethyl acetate with gentle heating to aid dissolution. The solution was extracted with water (2 × 25 mL) and brine (1 × 25 mL), dried over MgSO<sub>4</sub>, filtered, and concentrated to a solid. This was recrystallized from 40 mL of ethyl acetate to give 1.3 g (54%) of colorless crystals. <sup>1</sup>H NMR (400 MHz, DMSO-*d*<sub>6</sub>) δ 12.95 (br s, 1H), 9.44 (br s, 1H), 7.89 (d, *J* = 7.1 Hz, 1H), 7.30 (t, *J* = 7.2 Hz, 1H), 7.11 (m, 2H), 7.03 (t, *J* = 4.5 Hz, 1H), 6.69 (m, 2H), 2.29 (s, 3H), 2.10 (s, 3H); MS (ESI) (M + H)<sup>+</sup> at *m/z* 242.

**2-[(2,3-Dimethylphenyl)oxalylamino]benzoic Acid (1).** To an ice-cooled solution of **6** (R = 2,3-dimethyl) (343 mg, 1.55 mmol) and triethylamine (503 μL, 3.56 mmol) in dichloromethane (5 mL) was added ethyloxalyl chloride (401 μL, 3.56 mmol) over 30 min. The reaction mixture was warmed to ambient temperature and stirred for 16 h. The reaction mixture was then treated with 1 M HCl (10 mL) and extracted with dichloromethane (2 × 15 mL). The combined extracts were washed with brine, dried over Na<sub>2</sub>SO<sub>4</sub>, filtered, and concentrated in vacuo. The residue was dissolved in 5 mL of methanol, and 4.5 mL (4.5 mmol) of 1 N NaOH(aq) was added. After being stirred for 2 h at ambient temperature, the basic reaction mixture was diluted with 1 M HCl (10 mL). The product was isolated via reverse-phase HPLC to provide 235 mg (48%) of **1** as a light-brown solid. <sup>1</sup>H NMR (300 MHz, DMSO-*d*<sub>6</sub>, a 1:1 mixture of rotamers) δ [7.94 (d, *J* = 7.5 Hz), 7.81 (dd, *J* = 7.8, 1.7 Hz), 1H in total], [7.55 (td, *J* = 7.8, 1.7 Hz), 7.48 (td, *J* = 7.8, 1.7 Hz), 1H in total], [7.41 (td, *J* = 7.8, 1.1 Hz), 7.35 (td, *J* = 7.4, 1.4 Hz), 1H in total], [7.29 (dd, *J* = 7.8, 1.4 Hz), 7.24 (dd, *J* = 6.1 Hz), 1H in total], [7.19 (d, *J* = 7.8 Hz), 7.08 (d, *J* = 7.8 Hz), 1H in total], 7.14 (d, *J* = 7.5 Hz, 1H), [7.03 (d, *J* = 7.1 Hz), 6.83 (d, *J* = 7.1, 1.0 Hz), 1H in total]; MS (ESI) (M + H)<sup>+</sup> at *m/z* 314; HRMS calcd for (M + H)<sup>+</sup> C<sub>17</sub>H<sub>15</sub>N<sub>1</sub>O<sub>5</sub> 314.1028, found 314.1037; analytical HPLC *t*<sub>R</sub> = 6.16 min (A), *t*<sub>R</sub> = 1.75 min (B).

**2-(Naphthalen-2-yloxyalylamino)benzoic Acid (8a) (Method A).** <sup>1</sup>H NMR (300 MHz, DMSO-*d*<sub>6</sub>) δ 7.98–7.82 (m, 4H), 7.72–7.62 (m, 3H), 7.58–7.45 (m, 4H); MS (ESI) (M + H)<sup>+</sup> at *m/z* 336; HRMS calcd for (M + H)<sup>+</sup> C<sub>19</sub>H<sub>14</sub>N<sub>1</sub>O<sub>5</sub> 336.0872, found 336.0879.

**2-[(7-Hydroxynaphthalen-1-yl)oxalylamino]benzoic Acid (8b).** A solution of 2-[(7-benzyloxy-1-naphthyl)(carboxy-carbonyl)amino]benzoic acid (method A from 7-benzyloxy-1-naphthalenamine) (74 mg, 0.17 mmol) in dioxane (1 mL) at room temperature was treated with 10% Pd/C (10 mg) and 60% HClO<sub>4</sub> (1 drop), stirred under H<sub>2</sub> (1 atm) for 4 h, and filtered through diatomaceous earth (Celite). The filter cake was washed with ethyl acetate, and the combined filtrates were concentrated. The concentrate was purified by reverse-phase HPLC to provide **8b** as a mixture of rotamers. <sup>1</sup>H NMR (300 MHz, DMSO-*d*<sub>6</sub>) δ 10.04 (br s, 1H), 9.91 (br s, 1H), 7.92–7.75 (m, 3H), 7.64–7.14 (m, 6H), [7.11 (dd, *J* = 8.8, 2.4 Hz), 6.92 (d, *J* = 7.8 Hz), 1H in total]; MS (ESI) (M + Na)<sup>+</sup> at *m/z* 374; HRMS calcd for (M + Na)<sup>+</sup> C<sub>19</sub>H<sub>13</sub>N<sub>1</sub>O<sub>6</sub> 374.0641, found 374.0628; analytical HPLC *t*<sub>R</sub> = 5.78 min (A), *t*<sub>R</sub> = 1.53 min (B).

**2-[Oxalyl-(5,6,7,8-tetrahydronaphthalen-1-yl)amino]benzoic Acid (8c) (Method A).** <sup>1</sup>H NMR (500 MHz, DMSO-*d*<sub>6</sub>, a mixture of rotamers) δ [7.92 (d, *J* = 7.5 Hz), 7.81 (dd, *J* = 7.8, 1.9 Hz), 1H in total], [7.54 (dt, *J* = 7.8, 1.6 Hz), 7.48 (dt, *J* = 7.5, 1.6 Hz), 1H in total], [7.41 (dt, *J* = 7.8, 1.5 Hz), 7.35 (dt, *J* = 7.5, 1.3 Hz), 1H in total], 7.24–7.03 (m, 3H), [6.96 (d, *J* = 7.2 Hz), 6.84 (d, *J* = 8.1 Hz), 1H in total], 3.11 (td, *J* = 16.8, 5.0 Hz, 1H), 2.81 (br s, 1H), 2.75 (m, 2H), 1.89–1.63

(br m, 3H), 1.62–1.54 (m, 1H); MS (ESI) (M + H)<sup>+</sup> at *m/z* 340; HRMS calcd for (M + H)<sup>+</sup> C<sub>19</sub>H<sub>17</sub>N<sub>1</sub>O<sub>5</sub> 340.1185, found 340.1196.

**2-[(2-Ethylphenyl)oxalylamino]benzoic Acid (8d) (Method B).** <sup>1</sup>H NMR (400 MHz, DMSO-*d*<sub>6</sub>, a mixture of rotamers) δ [7.92 (d, *J* = 8.0 Hz), 7.82 (d, *J* = 7.8 Hz), 1H in total], [7.56 (t, *J* = 7.6 Hz), 7.49 (t, *J* = 7.6 Hz), 1H in total], 7.44–7.27 (m, 4H), [7.21–7.09 (m), 6.84 (d, *J* = 6.8 Hz), 2H in total], 2.74–2.60 (m, 2H), 0.94 (t, *J* = 7.3 Hz, 3H). MS (ESI) (M + H)<sup>+</sup> at *m/z* 314, (M + NH<sub>4</sub>)<sup>+</sup> at *m/z* 331; HRMS calcd for (M + H)<sup>+</sup> C<sub>17</sub>H<sub>16</sub>N<sub>1</sub>O<sub>5</sub> 314.1028, found 314.1021.

**2-[(2-Isopropylphenyl)oxalylamino]benzoic Acid (8e) (Method B).** <sup>1</sup>H NMR (400 MHz, DMSO-*d*<sub>6</sub>, a mixture of rotamers) δ [7.96 (d, *J* = 8.0 Hz), 7.82 (d, *J* = 8.0 Hz), 1H in total], 7.62–7.14 (m, 6H), [7.06 (d, *J* = 8.0 Hz), 6.80 (d, *J* = 8.0 Hz), 1H in total], 3.19 (br m, 1H), 1.16 (d, *J* = 8.0 Hz, 1H). MS (ESI) (M – H)<sup>–</sup> at *m/z* 326; HRMS calcd for (M – H)<sup>–</sup> C<sub>18</sub>H<sub>16</sub>N<sub>1</sub>O<sub>5</sub> 326.1029, found 326.1024.

**2-[(2-Benzylphenyl)oxalylamino]benzoic Acid (8f) (Method B).** <sup>1</sup>H NMR (400 MHz, DMSO-*d*<sub>6</sub>, a mixture of rotamers) δ [7.92 (d, *J* = 4.0 Hz), 7.80 (dd, *J* = 7.8, 4.0 Hz), 1H in total], 7.50–7.39 (m, 2H), 7.36–7.02 (m, 9H), [6.95 (d, *J* = 8.0 Hz), 6.79 (d, *J* = 8.0 Hz), 1H in total], 4.23 (d, *J* = 15.9 Hz, 1H), 3.87 (d, *J* = 15.9 Hz, 1H); MS (ESI) (M + NH<sub>4</sub>)<sup>+</sup> at *m/z* 393; HRMS calcd for (M + H)<sup>+</sup> C<sub>22</sub>H<sub>18</sub>N<sub>1</sub>O<sub>5</sub> 376.1185, found 376.1177.

**2-[[2-(2-Hydroxyethyl)phenyl]oxalylamino]benzoic Acid (8g) (Method B).** <sup>1</sup>H NMR (300 MHz, DMSO-*d*<sub>6</sub>) δ [7.98 (dd, *J* = 7.5, 1.8 Hz), 7.85 (dd, *J* = 7.5, 1.8 Hz), 1H in total], 7.58–7.22 (m, 6H), [7.18 (d, *J* = 7.5 Hz) and 6.83 (d, *J* = 7.5 Hz), 1H in total], 4.44 (t, *J* = 6.9 Hz, 2H), 3.12–2.92 (m, 2H); MS (ESI) (M + H)<sup>+</sup> at *m/z* 330; HRMS calcd for (M + H)<sup>+</sup> C<sub>17</sub>H<sub>16</sub>N<sub>1</sub>O<sub>6</sub> 330.0977, found 330.0986.

**2-[[2-(2-Carbamoylviny]phenyl]oxalylamino]benzoic Acid (8h) (Method B).** <sup>1</sup>H NMR (300 MHz, DMSO-*d*<sub>6</sub>, a mixture of rotamers) δ 8.05–7.92 (m, 1H), 7.76 (d, *J* = 15.6 Hz, 1H), 7.86–7.23 (m, 7H), 7.17–7.08 (m, 1H), 7.05–6.79 (m, 1H), 6.72–6.53 (three sets of d, *J* = 15.6 Hz, 1H in total); MS (ESI) (M + H)<sup>+</sup> at *m/z* 355; HRMS calcd for (M + H)<sup>+</sup> C<sub>18</sub>H<sub>15</sub>N<sub>2</sub>O<sub>6</sub> 355.0930, found 355.0921.

**2-[Oxalyl(2-piperidin-1-ylphenyl)amino]benzoic Acid (8i) (Method B).** <sup>1</sup>H NMR (400 MHz, DMSO-*d*<sub>6</sub>, a mixture of rotamers) δ 7.83 (d, *J* = 7.2 Hz, 1H), 7.53 (t, *J* = 7.2 Hz, 1H), 7.43–7.30 (m, 2H), 7.38 (t, *J* = 8.4 Hz, 1H), 7.24–7.08 (m, 2H), 6.99 (br m, 1H), 2.86 (br m, 4H), 1.68–1.38 (m, 6H); MS (ESI) (M + H)<sup>+</sup> at *m/z* 369; HRMS calcd for (M + H)<sup>+</sup> C<sub>20</sub>H<sub>20</sub>N<sub>2</sub>O<sub>5</sub> 369.1450, found 369.1466.

**General Synthesis of *p*-Aminophenylalanine Derivatives, Exemplified by 12a. 2-Acetylamino-3-(4-aminonaphthalen-1-yl)acrylic Acid Methyl Ester (9, Ar = 2-Naphthalene).** To a mixture of 4-bromo-1-naphthylamine (2.5 g, 11.3 mmol), Pd(OAc)<sub>2</sub> (140 mg, 0.63 mmol), and P(*o*-tolyl)<sub>3</sub> (570 mg, 1.87 mmol) in anhydrous *N,N*-dimethylformamide (10 mL) in a pressure tube was added methyl 2-acetamidoacrylate (2.1 g, 14.7 mmol) and triethylamine (5.3 mL, 37.5 mmol). The mixture was flushed with N<sub>2</sub> for 3 min and then sealed and heated at 110 °C for 4 h. The reaction mixture was cooled to ambient temperature and then partitioned between ethyl acetate and water. The aqueous layer was extracted once with ethyl acetate, and the combined organic layers were washed with brine, dried (Na<sub>2</sub>SO<sub>4</sub>), filtered, concentrated in vacuo. The crude residue was purified via silica gel chromatography, eluting with ethyl acetate to provide 2.5 g (76%) of compound **9** as a yellow solid. <sup>1</sup>H NMR (400 MHz, DMSO-*d*<sub>6</sub>) δ 9.34 (s, 1H), 8.15 (d, *J* = 8.0 Hz, 1H), 7.90 (d, *J* = 8.0 Hz, 1H), 7.78 (s, 1H), 7.63 (d, *J* = 8.0 Hz, 1H), 7.51 (t, *J* = 7.6 Hz, 1H), 7.42 (t, *J* = 7.6 Hz, 1H), 6.72 (d, *J* = 8.0 Hz, 1H), 6.29 (s, 2H), 3.73 (s, 3H), 1.94 (s, 3H); MS (ESI) (M + H)<sup>+</sup> at *m/z* 285.

**2-Acetylamino-3-(4-aminonaphthalen-1-yl)propionic acid (10).** To a solution of **9** (2.5 g, 8.8 mmol) in 1:1 (v/v) ethyl acetate/methanol (50 mL) under N<sub>2</sub> was added Pd/C (10%, 250 mg). The reaction flask was capped with a hydrogen balloon and heated at 60 °C for 18 h. The mixture was filtered through



diatomaceous earth, and the filter bed was washed with 1:1 (v/v) ethyl acetate/methanol ( $2 \times 25$  mL). The filtrate was concentrated in vacuo to provide the methyl propionate (2.5 g, 100%). The methyl ester was dissolved in methanol (50 mL), and then 3 N NaOH (4.75 mL, 14.3 mmol) was added dropwise. After the reaction mixture was stirred for 3 h at ambient temperature, the methanol was removed in vacuo and the remaining aqueous solution was acidified to pH  $\sim$ 4.5 with 3 N HCl. The mixture was concentrated to dryness in vacuo, taken up in 10% (v/v) methanol/dichloromethane (25 mL), and filtered through diatomaceous earth. The filter cake was washed with an additional 10% (v/v) methanol/dichloromethane (25 mL). The filtrate was concentrated under reduced pressure to provide acid **10** as a brown solid (1.75 g, 74%).  $^1\text{H NMR}$  (400 MHz, DMSO- $d_6$ )  $\delta$  8.17 (d,  $J = 8.0$  Hz, 1H), 8.08 (d,  $J = 8.0$  Hz, 1H), 7.99 (d,  $J = 8.0$  Hz, 1H), 7.48 (t,  $J = 7.8$  Hz, 1H), 7.38 (t,  $J = 7.8$  Hz, 1H), 7.12 (d,  $J = 7.8$  Hz, 1H), 6.60 (d,  $J = 7.8$  Hz, 1H), 1.77 (s, 3H), 4.45 (td,  $J = 9.2, 4.8$  Hz, 1H), 3.43 (dd,  $J = 14.0, 4.8$  Hz, 1H), 3.05 (dd,  $J = 14.0, 9.2$  Hz, 1H); MS (ESI) (M + H) $^+$  at  $m/z$  273.

**2-Acetylamino-3-(4-aminonaphthalen-1-yl)-N-pentylpropionamide (11).** A solution of **10** (500 mg, 1.84 mmol), 1-[3-(dimethylamino)propyl]-3-ethylcarbodiimide hydrochloride (EDCI) (493 mg, 2.57 mmol), 1-hydroxybenzotriazole hydrate (360 mg, 2.21 mmol), and *n*-pentylamine (320  $\mu\text{L}$ , 2.75 mmol) in anhydrous *N,N*-dimethylformamide (10 mL) was adjusted to pH  $\sim$ 6 by the addition of triethylamine, and then the reaction mixture was stirred for 5 h at ambient temperature. The reaction mixture was diluted with water and extracted with ethyl acetate ( $3 \times 15$  mL). The combined ethyl acetate layers were washed with water and brine, dried over  $\text{Na}_2\text{SO}_4$ , filtered, and concentrated in vacuo. The product was purified via silica gel chromatography, eluting with 5% (v/v) MeOH/EtOAc to provide amide **11** as a yellow solid (552 mg, 88%).  $^1\text{H NMR}$  (400 MHz, DMSO- $d_6$ )  $\delta$  8.15 (d,  $J = 8.0$  Hz, 1H), 8.07 (s, 1H), 8.04 (s, 1H), 7.87 (t,  $J = 5.9$  Hz, 1H), 7.45 (t,  $J = 8.0$  Hz, 1H), 7.36 (t,  $J = 8.0$  Hz, 1H), 7.08 (d,  $J = 8.0$  Hz, 1H), 6.58 (d,  $J = 8.0$  Hz, 1H), 5.52 (s, 2H), 4.27 (q,  $J = 5.9$  Hz, 1H), 3.28 (dd,  $J = 14.0, 5.9$  Hz, 1H), 2.94–3.06 (m, 3H), 1.77 (s, 3H), 1.18–1.39 (m, 4H), 1.14 (heptet,  $J = 7.8$  Hz, 2H), 0.84 (t,  $J = 7.5$  Hz, 3H); MS (ESI) (M + H) $^+$  at  $m/z$  342.

**2-[4-(2-Acetylamino-2-pentylcarbamoyl)ethyl]naphthalen-1-yl]oxalylamino]benzoic Acid (12a).** To a stirred suspension of **11** (552 mg, 1.62 mmol) and diphenyliodonium 2-carboxylate monohydrate (580 mg, 1.78 mmol) in *N,N*-dimethylformamide (10 mL) was added anhydrous  $\text{Cu}(\text{OAc})_2$  (14.6 mg, 0.081 mmol). The mixture was heated at 95  $^\circ\text{C}$  for 1.5 h. The reaction mixture was then concentrated in vacuo, and the crude residue was purified by reverse-phase preparative HPLC to give 2-[4-(2-acetylamino-2-pentylcarbamoyl)ethyl]naphthalen-1-ylamino]benzoic acid as a light-brown solid (619 mg, 83%).

To an ice cooled, stirred solution of above benzoic acid (619 mg, 1.34 mmol) and triethylamine (680  $\mu\text{L}$ , 5.13 mmol) in dichloromethane (10 mL) was added ethyloxalyl chloride (452  $\mu\text{L}$ , 4.04 mmol) slowly over 30 min. The reaction mixture was warmed to ambient temperature and stirred for 16 h. After this time, 1 N HCl (10 mL) was added and the mixture was extracted with dichloromethane ( $2 \times 20$  mL). The combined dichloromethane layers were washed with brine, dried over  $\text{Na}_2\text{SO}_4$ , filtered, and concentrated in vacuo to give the crude 2-[4-(2-acetylamino-2-pentylcarbamoyl)ethyl]naphthalen-1-yl]ethoxyoxalylamino]benzoic acid.

To a solution of above crude ester (950 mg) in methanol (7 mL) at ambient temperature was added 1 N NaOH (3.9 mL). The basic mixture was stirred at ambient temperature for 2 h, and then 1 N HCl (10 mL) was added. The product was purified by reverse-phase preparative HPLC to provide 210 mg of compound **12a** as a light-brown solid (0.39 mmol, 29% yield over two steps).  $^1\text{H NMR}$  (400 MHz, DMSO- $d_6$ , a mixture of rotamers)  $\delta$  13.13 (s, 1H), 8.43 (t,  $J = 7.8$  Hz, 1H), 8.32 (d,  $J = 8.4$  Hz, 1H), 8.22 (dd,  $J = 8.4, 2.8$  Hz, 1H), [8.18 (d,  $J = 8.4$  Hz), 8.08 (d,  $J = 8.4$  Hz), 1H in total], 8.01–7.83 (m, 3H), 7.75–7.12 (m, 5H), 6.86–6.80 (m, 1H), 4.58 (q,  $J = 7.4$  Hz,

1H), 3.67–2.82 (m, 6H), [(1.81, s), (1.78, s), (1.75, s), 3H in total], 1.39–1.00 (m, 4H), 0.92–0.69 (m, 3H); MS (ESI) (M + H) $^+$  at  $m/z$  534; HRMS calcd for (M + H) $^+$   $\text{C}_{29}\text{H}_{32}\text{N}_3\text{O}_7$  534.2240, found 534.2246; analytical HPLC  $t_{\text{R}} = 6.66$  min (A),  $t_{\text{R}} = 1.84$  min (B).

**2-[4-(2-Acetylamino-2-pentylcarbamoyl)ethyl]-2-ethylphenyl]oxalylamino]benzoic Acid (12b).** Light-brown solid;  $^1\text{H NMR}$  (300 MHz, DMSO- $d_6$ , a mixture of rotamers)  $\delta$  8.17–8.01 (m, 1H), 7.98–7.74 (m, 2H), 7.60–6.93 and 6.83–6.71 (m, 6H), 4.52–4.36 (m, 1H), 3.07–2.84 (m, 4H), 2.83–2.53 (m, 2H), 1.87 (s, 3H), 1.42–1.01 (m, 9H), 0.93 (t,  $J = 7.7$  Hz, 2H), 0.88–0.74 (m, 3H); MS (ESI) (M + H) $^+$  at  $m/z$  512; HRMS calcd for (M + H) $^+$   $\text{C}_{27}\text{H}_{34}\text{N}_3\text{O}_7$  512.2397, found 512.2416; analytical HPLC  $t_{\text{R}} = 6.49$  min (A),  $t_{\text{R}} = 1.82$  min (B).

**N-Acetyl-4-[(carboxycarbonyl)(2-carboxyphenyl)amino]-3-isopropyl-N-pentylphenylalaninamide (12c).** Light-brown solid;  $^1\text{H NMR}$  (500 MHz, DMSO- $d_6$ , a mixture of rotamers)  $\delta$  7.90–8.16 (m, 2H), 6.73–7.60 (m, 4H), 4.40–4.52 (m, ca. 0.6 H), 2.7–3.3 (m, ca. 5.4H), 1.77 and 1.74 (s, 3H), 1.1–1.41 (m, 11H), 0.62–0.90 (m, 3H); MS (ESI) (M + H) $^+$  at  $m/z$  526; HRMS calcd for (M + H) $^+$   $\text{C}_{28}\text{H}_{35}\text{N}_3\text{O}_7$  526.2553, found 526.2579; analytical HPLC  $t_{\text{R}} = 6.86$  min (A),  $t_{\text{R}} = 1.89$  min (B).

**N-Acetyl-4-[(carboxycarbonyl)(2-carboxyphenyl)amino]-N-pentyl-3-(2-hydroxyethane)phenylalaninamide (12d).**  $^1\text{H NMR}$  (300 MHz, DMSO- $d_6$ , a mixture of rotamers)  $\delta$  8.14–7.58 (m, 3H), 7.52–6.85 (m, 6H), 4.80–4.30 (m, 3H), 3.60–3.79 (m, 2H), 3.04–2.64 (m, 6H), 1.82–1.73 (multiple s, 3H in total), 1.40–1.10 (m, 4H), 0.84 (t,  $J = 7.4$  Hz, 3H); MS (ESI) (M + H) $^+$  at  $m/z$  528; HRMS calcd for (M + Na) $^+$   $\text{C}_{27}\text{H}_{33}\text{N}_3\text{O}_8\text{Na}$  550.2165, found 550.2187; analytical HPLC  $t_{\text{R}} = 5.60$  min (A),  $t_{\text{R}} = 1.58$  min (B).

**2-[4-(2-Acetylamino-2-pentylcarbamoyl)ethyl]-2-piperidin-1-ylphenyl]oxalylamino]benzoic Acid (12e).** Light-brown solid;  $^1\text{H NMR}$  (500 MHz, DMSO- $d_6$ , a mixture of rotamers)  $\delta$  7.90–8.16 (m, 2H), 6.73–7.60 (m, 4H), 4.40–4.52 (br m, ca. 0.6 H), 2.7–3.3 (m, ca. 8.4H), 1.77 and 1.74 (s, 3H), 1.19–1.62 (m, 18H); MS (ESI) (M + H) $^+$  at  $m/z$  567; HRMS calcd for (M + H) $^+$   $\text{C}_{30}\text{H}_{39}\text{N}_4\text{O}_7$  567.2819, found 567.2844; analytical HPLC  $t_{\text{R}} = 5.52$  min (A),  $t_{\text{R}} = 1.52$  min (B).

**3-(4-Amino-3-iodophenyl)-2-methanesulfonylamino-N-pentylpropionamide (14).** To a stirred solution of 3-(4-aminophenyl)-2-(*S*)-methanesulfonylamino-*N*-pentylpropionamide (**13**) (1.1 g, 3.4 mmol) in acetic acid (5 mL) was added NaI (0.59 g, 3.9 mmol) followed by the addition of chloramines-T trihydrate (1.1 g, 3.9 mmol). The solution was stirred for 1 h, concentrated under reduced pressure, diluted with aqueous  $\text{Na}_2\text{S}_2\text{O}_4$  solution, and partitioned between EtOAc and aqueous  $\text{NaHCO}_3$ . The organic layer was washed with brine, dried ( $\text{Na}_2\text{SO}_4$ ), filtered, concentrated under reduced pressure, and purified on silica gel, eluting with 20% EtOAc/hexanes to provide 0.78 g (1.7 mmol, 50%) of **14** as a light-yellow solid.  $^1\text{H NMR}$  (300 MHz, DMSO- $d_6$ )  $\delta$  7.83 (t,  $J = 5.6$  Hz, 1H), 7.32 (d,  $J = 2.2$  Hz, 1H), 6.85 (dd,  $J = 7.8, 2.2$  Hz, 1H), 6.63 (d,  $J = 7.8$  Hz, 1H), 4.18 (q,  $J = 7.5$  Hz, 1H), 3.04 (t,  $J = 6.3$  Hz, 1H), 2.94 (t,  $J = 6.3$  Hz, 1H), 2.82 (s, 3H), 2.66 (dd,  $J = 13.8, 6.0$  Hz, 1H), 2.54 (dd,  $J = 13.8, 6.0$  Hz, 1H), 1.40–1.10 (m, 6H), 0.68 (t,  $J = 7.4$  Hz, 3H); MS (ESI) (M + H) $^+$  at  $m/z$  454.

**2-[2-(2-Carbamoylvinyl)-4-(2-methanesulfonylamino-2-pentylcarbamoyl)ethyl]phenylamino]benzoic Acid (16).** To a stirred suspension of **14** (214 mg, 0.47 mmol) and DPIC (168 mg, 0.49 mmol) in *N,N*-dimethylformamide (5 mL) was added anhydrous  $\text{Cu}(\text{OAc})_2$  (7.3 mg, 0.040 mmol). The resulting mixture was heated to 95  $^\circ\text{C}$  for 90 min. The reaction mixture was then concentrated under reduced pressure. The residue was further concentrated to a constant weight on an oil pump to give 2-[2-iodo-4-(2-methanesulfonylamino-2-pentylcarbamoyl)ethyl]phenylamino]benzoic acid (**15**) as a light-brown solid (306 mg), which was used directly without further purification.

To a mixture of **15** (306 mg, 0.51 mmol),  $\text{Pd}(\text{OAc})_2$  (6 mg, 0.026 mmol),  $\text{P}(o\text{-toly})_3$  (23 mg, 0.80 mmol) in anhydrous *N,N*-dimethylformamide (10 mL) in a pressure tube was added



acrylamide (66 mg, 0.93 mmol) and triethylamine (0.25 mL, 1.79 mmol). The mixture was flushed with N<sub>2</sub> for 3 min before it was sealed and heated to 90 °C for 16 h. The reaction mixture was cooled to ambient temperature, and the solvent was removed on a SpeedVac. The residue was taken up in methanol and purified on a Gilson preparative HPLC to provide 153 mg of **16** (0.28 mmol, 60%) as a yellow solid. <sup>1</sup>H NMR (300 MHz, DMSO-*d*<sub>6</sub>) δ 9.53 (s, 1H), 8.00 (t, *J* = 5.6 Hz, 1H), 7.90 (dd, *J* = 8.1, 1.8 Hz, 1H), 7.64–7.53 (m, 2H), 7.54 (d, *J* = 15.6 Hz, 1H), 7.33 (dd, *J* = 7.2, 1.8 Hz, 1H), 7.31 (d, *J* = 7.2 Hz, 1H), 7.09 (br s, 1H), 6.75 (td, *J* = 7.5, 0.9 Hz, 1H), 6.70 (d, *J* = 8.7 Hz, 1H), 6.61 (d, *J* = 15.6 Hz, 1H), 4.02 (q, *J* = 7.2 Hz, 1H), 3.15–2.76 (m, 4H), 2.65 (s, 3H), 1.36–1.16 (m, 6H), 0.81 (t, *J* = 7.2 Hz, 1H); MS (ESI) (M + H)<sup>+</sup> at *m/z* 517.

**2-{{2-(2-Carbamoylvinyl)-4-(2-(S)-methanesulfonylamino-2-pentylcarbamoyl)ethyl}phenyl}oxalylamino}benzoic Acid (17).** Method B from **16**. Light-yellow solid; <sup>1</sup>H NMR (300 MHz, DMSO-*d*<sub>6</sub>, a mixture of rotamers) δ 8.05–7.92 (m, 1H), 7.79 (d, *J* = 15.6 Hz, 1H), 7.86–7.23 (m, 7H), 7.17 (d, *J* = 7.8 Hz, 1H), 7.05 and 6.79 (d, *J* = 8.4 Hz, 1H in total), 6.74–6.53 (three sets of d, *J* = 15.6 Hz, 1H in total), 4.38 (m, 1H), 3.10–2.69 (m, 4H), 2.43 (s, 3H), 1.11–1.42 (m, 6H), 0.90–0.77 (m, 3H); MS (ESI) (M + H)<sup>+</sup> at *m/z* 589; HRMS calcd for (M + H)<sup>+</sup> C<sub>27</sub>H<sub>33</sub>N<sub>4</sub>O<sub>9</sub>S 589.1968, found 589.1979; analytical HPLC *t*<sub>R</sub> = 4.89 min (A), *t*<sub>R</sub> = 1.35 min (B).

**2-{{4-((S)-2-tert-Butoxycarbonylamino-2-pentylcarbamoyl)ethyl}phenyl}oxalylamino}benzoic Acid (18).** White solid; <sup>1</sup>H NMR (300 MHz, DMSO-*d*<sub>6</sub>, a mixture of rotamers) δ 7.86 (s, 1H), 7.55–7.41 (m, 2H), 7.38 (br d, *J* = 6.9 Hz, 1H), 7.17 (d, *J* = 8.1 Hz, 2H), 7.09 (d, *J* = 8.1 Hz, 2H), 6.71 (d, *J* = 8.7 Hz, 1H), 4.00–4.10 (br m, 1H), 3.06–2.95 (br m, 2H), 2.89–2.80 (br m, 2H), 1.42–1.14 (m, 6H), 1.28 (s, 9H), 0.85 (t, *J* = 6.9 Hz, 3H); MS (ESI) (M + H)<sup>+</sup> at *m/z* 542; HRMS calcd for (M + H)<sup>+</sup> C<sub>28</sub>H<sub>35</sub>N<sub>3</sub>O<sub>8</sub> 542.2502, found 542.2510.

**2-{{4-(2-(S)-Amino-2-pentylcarbamoyl)ethyl}phenyl}oxalylamino}benzoic Acid (19).** Light-brown oil; <sup>1</sup>H NMR (300 MHz, DMSO-*d*<sub>6</sub>, a mixture of rotamers) δ 8.35–8.07 (m, 3H), 7.96–7.85 (m, 1H), 7.68–7.36 (m, 3H), 7.25–7.17 (m, 2H), 3.95–3.84 (m, 1H), 3.13–2.87 (m, 4H), 1.40–1.08 (m, 6H), 0.90–0.77 (m, 3H); MS (ESI) (M + H)<sup>+</sup> at *m/z* 442.

**2-{{4-(2-(S)-Acetylamino-2-pentylcarbamoyl)ethyl}phenyl}oxalylamino}benzoic Acid (20).** White solid; <sup>1</sup>H NMR (300 MHz, DMSO-*d*<sub>6</sub>, a mixture of rotamers) δ 8.12–8.03 (m, 1H), 7.97–7.82 (m, 2H), 7.66–7.32 (m, 3H), 7.28–7.14 (m, 3H), 4.42 (q, *J* = 6.0 Hz, 1H), 3.06–2.85 (m, 3H), 2.80–2.66 (m, 1H), 1.75 (s, 3H), 1.40–1.10 (m, 6H), 0.86–0.78 (m, 3H); MS (ESI) (M + H)<sup>+</sup> at *m/z* 484; HRMS calcd for (M + H)<sup>+</sup> C<sub>25</sub>H<sub>30</sub>N<sub>3</sub>O<sub>7</sub> 484.2084, found 484.2079.

**2-{{4-(2-(S)-Methanesulfonylamino-2-pentylcarbamoyl)ethyl}phenyl}oxalylamino}benzoic Acid (21).** White solid; <sup>1</sup>H NMR (300 MHz, DMSO-*d*<sub>6</sub>, a mixture of rotamers) δ 7.86 (s, 1H), 7.55–7.41 (m, 2H), 7.38 (br d, *J* = 6.9 Hz, 1H), 7.17 (d, *J* = 8.1 Hz, 2H), 7.09 (d, *J* = 8.1 Hz, 2H), 6.71 (d, *J* = 8.7 Hz, 1H), 4.00–4.10 (br m, 1H), 3.06–2.95 (br m, 2H), 2.89–2.80 (br m, 2H), 2.84 (s, 3H), 1.42–1.14 (m, 6H), 0.85 (t, *J* = 6.9 Hz, 3H); MS (ESI) (M + H)<sup>+</sup> at *m/z* 520; HRMS calcd for (M + H)<sup>+</sup> C<sub>24</sub>H<sub>30</sub>N<sub>3</sub>O<sub>8</sub> 520.1753, found 520.1746.

**NMR-Based Screening.** Human PTP1B (residues 1–288) was cloned into the pGEX-5X vector (Amersham Pharmacia) and expressed in *E. coli* BL21(DE3) cells. The final protein construct used for the NMR studies was 292 residues comprising the following amino acid sequence:

```

4 1
GFSH MEMEKEFEQI DKSQSWAAIY QDIRHEASDF PCRVAKLKPN KNNRNYRDVVS 50
PFDSRIKHL QEDNDYINAS LIKMEEAQRS YILTQGLPN TCGHFWEVWV 100
EQKSRGVVML NRVMEKGLSK CAQYWPQKEE KEMIFEDTNL KLTLSIEDIK 150
SYTYVRQLEL ENLTTQETRE ILHFHYTTWP DFGVPESPAS FLNLFKVVRE 200
SGLSPEHPG VVVCASAGI RSGTFCLADT CLLMDKRKD PSSVDIKKVL 250
LDMRFRMGL IQTAEQLRFS YLAVIEGAKF IMGD 288

```

Two point mutations exist in the construct (E252D and D265E,

highlighted in yellow), along with four additional N-terminal residues (GFSH) that remain after cleavage of the GST fusion.

Uniformly <sup>15</sup>N-labeled and <sup>13</sup>CH<sub>3</sub>(IVLM)-labeled PTP1B was prepared by growing the bacteria on a minimal medium containing 1 g/L of <sup>15</sup>NH<sub>4</sub>Cl (Cambridge Isotopes) or by adding 100:100:50 mg/L of <sup>13</sup>C-γ-methionine/3,3'-<sup>13</sup>C-α-ketoglutarate/3-<sup>13</sup>C-α-ketobutyrate<sup>18</sup> 1 h before induction with 1 mM IPTG. Carbenicillin (0.1 mg/mL) was used as the selection agent. In addition to the standard salts, metals, and vitamins, the media contained the following additives (g/L of culture): Ala (0.5), Arg (0.4), Asp (0.4), Cys (0.05), Glu (0.65), Gln (0.4), Gly (0.55), His (0.1), Lys (0.42), Phe (0.13), Pro (0.1), Ser (2.1), Thr (0.23), Tyr (0.17), adenine (0.5), guanosine (0.65), thymine (0.2), uracil (0.5), cytosine (0.2), sodium acetate (1.5), and succinic acid (1.5). The cell pellets were resuspended in a buffer containing 10 mM sodium phosphate (pH 7.4) and 150 mM NaCl (PBS buffer). The cells were then lysed using a microfluidizer (Microfluidics International), and the resulting lysate was clarified via centrifugation at 76000*g* for 10 min. The clarified cell lysate was loaded onto a glutathione Sepharose 4B column (Pharmacia), and the resin was washed with 20 column volumes of PBS buffer. The protein was eluted with 5 column volumes of a buffer containing 50 mM Tris (pH 8.0) and 10 mM reduced glutathione. The N-terminal GST fusion was cleaved with thrombin (1 U of thrombin/mg of PTP1B) at 4 °C for 72 h. Cleavage was monitored by SDS-PAGE analysis. The resulting solution was then concentrated and dialyzed to remove the glutathione (final dilution factor of 10<sup>-10</sup>) and loaded onto a glutathione Sepharose 4B column to remove the GST. The flow-through (containing PTP1B) was collected and dialyzed against NMR buffer (see below). Typical protein yields were 10–20 mg of PTP1B per liter of culture.

The NMR samples were composed of uniformly <sup>15</sup>N-labeled or <sup>13</sup>CH<sub>3</sub>(IVLM) PTP1B in an H<sub>2</sub>O/D<sub>2</sub>O (9/1) Tris-buffered solution (25 mM, pH 7.5) containing DTT (10 mM). Ligand binding was detected by acquiring sensitivity-enhanced <sup>1</sup>H/<sup>15</sup>N- or <sup>1</sup>H/<sup>13</sup>C-HSQC spectra<sup>25</sup> on 400 μL of PTP1B in the presence and absence of added compound. Protein concentrations were 300 and 25 μM for the <sup>15</sup>N- and <sup>13</sup>CH<sub>3</sub>(IVLM)-labeled samples, respectively. A Bruker sample changer was used on a Bruker AMX500 spectrometer equipped with a cryoprobe.<sup>26</sup> Compounds were individually tested at concentrations of 0.1–15.0 mM, and binding was determined by monitoring changes in the HSQC spectra. Dissociation constants were obtained for selected compounds by monitoring the chemical shift changes of the protein resonances as a function of ligand concentration. Data were fit using a single binding site model. A least-squares grid search was performed by varying the values of *K*<sub>d</sub> and the chemical shift of the fully saturated protein.

**Biological Assay.** The procedure for the pNPP assay has been described elsewhere.<sup>27</sup>

**X-ray Crystallographic Studies: Protein Production, Crystallization, and Data Collection.** The final concentration of the purified PTP1B protein (1–322) was 3–4 mg/mL and contained various amounts of reducing agents, normally 2–4 mM DTT. Crystals of PTP1B belonging to space group *P*3<sub>1</sub>21 (*a* = *b* = 88.4 Å, *c* = 104.5 Å) were grown routinely using the protocol described by Puius et al.<sup>22</sup> with the following changes. The buffers used in protein crystallization were degassed for approximately 30 min and then sparged with argon gas prior to their use for crystallization. This simple precaution extended the lifetime of the reactive cysteine (Cys215) in the active site and provided a more stable and structurally homogeneous conformation of the active site. This protocol also allowed the direct soaking of all the PTP1B inhibitors into the crystals. Soaking times ranged from 1 to 5 h and were normally no more than 2 h. Soaking was performed using 50 μL of the reservoir in the crystallization well and mixed with a 2–4 μL of stock (DMSO) solution of the compound at 100 μM. The soaking protocol was validated with a control compound, 2-(oxalylamino)-4,5,6,7-tetrahydrothieno[2,3-*c*]pyridine-3-carboxylic acid.<sup>17</sup> No significant differences were observed within an extended area (~20 Å) around the

active site when the structure obtained was compared with the one reported. The soaking protocol permitted the rapid structure determination of PTP1B/inhibitor complexes.

After the soaking period, crystals were transferred to a cryoprotectant solution for 5–10 s with rayon loops and exposed to the X-rays. The cryoprotectant solution consisted of 100 mM HEPES and 0.2 M magnesium acetate adjusted to pH 7.1 with NaOH at a 16% w/v concentration of PEG8000 with a 35% v/v concentration of glycerol. Crystallographic data were collected routinely in a conventional, in-house protein crystallography laboratory, and occasionally at sector 17 at the Advanced Photon Source (ID and BM lines of IMCA-CAT). The data collection hardware was a Mar Research image plate (180 mm), a Mar Research 345 mm image plate, or a Mar Research 165 mm CCD detector, all driven by the manufacturer's software. For a complete data set, 80 1° frames were collected at a crystal to detector distance of 80–90 mm. Exposure times were typically 10 min/frame. This strategy resulted in >95% completeness in the vast majority of the data sets with reducing *R* factors between 5% and 9%. Data were processed with HKL2000 and scaled with SCALEPACK or within HKL2000. Phase and map calculations were performed using XPLOR or CNX. The modeling and electron-density fitting software QUANTA was used to manipulate the models.

**Pharmacokinetic Analysis.** Experimental details for pharmacokinetic analysis were previously described.<sup>28</sup>

**In Vivo Study with ob/ob Diabetic Mouse Model.** To evaluate the effects of PTP1B inhibitors in ob/ob mice, compound **12d** was administered subcutaneously via osmotic minipumps. Briefly, male ob/ob mice and their lean litter mates of 5–6 weeks (average age) (The Jackson Laboratories) were acclimated to the animal research facilities for 5 days. They were weighed, and tail snip glucose levels were determined by the glucose oxidase method (Precision G glucose meter, Abbott Laboratories, North Chicago). The animals were randomized into five treatment groups based on their plasma glucose levels and body weight (animals with glucose levels between 250 and 400 mg/dL were used). Baseline plasma insulin samples were taken from a subset of the animals representing each treatment group randomized once (*n* = 10 ob/ob and *n* = 6 lean ob/+ litter mates; ELISA, ALPCO Diagnostics, Windham, NH). The five treatment groups were as follows: vehicle control, minipump (*n* = 10); **12d**, 30 mg/kg minipump (*n* = 10); **12d**, 120 mg/kg minipump (*n* = 10); rosiglitazone, 3 mg/kg minipump (*n* = 10); lean control, no minipump (*n* = 10).

On day 1, the Alzet minipumps (model 2001, 1  $\mu$ L/h, 7 days, 200  $\mu$ L reservoir) was primed and loaded with vehicle control (20% DMSO/80% PEG400) and drugs. Animals were then implanted with Alzet minipumps. The animals were continuously dosed sc from days 1–6. After the day 6 dosing, tail bleed glucose and insulin (ob/ob and ob/+ only) levels, as well as body weight, were determined under nonfasting conditions by 10:00 a.m.

**Acknowledgment.** We thank Elizabeth Everitt for determining the Caco-2 permeability, Bach Hickman and Kennan Marsh for obtaining the rat pharmacokinetic data, and Jamey Mack and Flora Huang for preparing the isotopically labeled proteins for the NMR-based screening.

## References

- Kruszynska, Y. T.; Olefsky, J. M. Cellular and Molecular Mechanisms of Non-Insulin Dependent Diabetes Mellitus. *J. Invest. Med.* **1996**, *44*, 413–428.
- Youngren, J. F.; Goldfine, I. D. The Molecular Basis of Insulin Resistance. *Sci. Med.* **1997**, *4*, 18–27.
- Olefsky, J. M.; Garvey, W. T.; Henry, R. R.; Brillon, D.; Matthai, S.; Friedenberg, G. R. Cellular Mechanisms of Insulin Resistance in Non-Insulin Dependent (Type II) Diabetes. *Am. J. Med.* **1988**, *85* (S5A), 86–105.
- Kahn, C. R. Insulin Action, Diabetogenes, and the Cause of Type II Diabetes. *Diabetes* **1994**, *43*, 1066–1084.
- Czech, M. P.; Corvera, S. Signaling Mechanisms That Regulate Glucose Transport. *J. Biol. Chem.* **1999**, *274*, 1865–1868.
- Olefsky, J. M. Insulin-Stimulated Glucose Transport, Minireview Series. *J. Biol. Chem.* **1999**, *274*, 1863.
- For reviews on PTP1B target validation, see the following. (a) Goldstein, B. J. Protein–Tyrosine Phosphate 1B (PTP1B): A Novel Therapeutic Target for Type 2 Diabetes Mellitus, Obesity and Related States of Insulin Resistance. *Curr. Drug Targets: Immune, Endocr. Metab. Disord.* **2001**, *1*, 265–276. (b) Zhang, Z.-Y. Protein Tyrosine Phosphatases: Prospects for Therapeutics. *Curr. Opin. Chem. Biol.* **2001**, *5*, 416–423. (c) Ukkola, O.; Santaniemi, M. Protein Tyrosine Phosphatase 1B: A New Target for the Treatment of Obesity and Associated Co-Morbidities. *J. Intern. Med.* **2002**, *251*, 467–475. (d) Cheng, A.; Dube, N.; Gu, F.; Tremblay, M. L. Coordinated Action of Protein Tyrosine Phosphatases in Insulin Signal Transduction. *Eur. J. Biochem.* **2002**, *269*, 1050–1059.
- Elchebly, M.; Payette, P.; Michaliszyn, E.; Cromlish, W.; Collins, S.; Loy, A. L.; Normandin, D.; Cheng, A.; Himms-Hagen, J.; Chan, C. C.; Ramachandran, C.; Gresser, M. J.; Tremblay, M. L.; Kennedy, B. P. Increased Insulin Sensitivity and Obesity Resistance in Mice Lacking the Protein–Tyrosine Phosphatase-1B Gene. *Science* **1999**, *283*, 1544–1548.
- Klaman, L. D.; Boss, O.; Peroni, O. D.; Kim, J. K.; Martino, J. L.; Zabolotny, J. M.; Moghal, N.; Lubkin, M.; Kim, Y.-B.; Sharpe, A. H.; Stricker-Krongrad, A.; Shulman, G. I.; Neel, B. G.; Kahn, B. B. Increased Energy Expenditure, Decreased Adiposity, and Tissue-Specific Insulin Sensitivity in Protein–Tyrosine Phosphatase 1B-Deficient Mice. *Mol. Cell. Biol.* **2000**, *20*, 5479–5489.
- Cheng, A.; Uetani, N.; Simoncic, P. D.; Chaubey, V. P.; Lee-Loy, A.; McGlade, C. J.; Kennedy, B. P.; Tremblay, M. L. Attenuation of Leptin Action and Regulation of Obesity by Protein Tyrosine Phosphatase 1B. *Dev. Cell* **2002**, *2*, 497–503.
- Zabolotny, J. M.; Bence-Hanulec, K. K.; Stricker-Krongrad, A.; Haj, F.; Wang, Y.; Minokoshi, Y.; Kim, Y. B.; Elmquist, J. K.; Tartaglia, L. A.; Kahn, B. B.; Neel, B. G. PTP1B Regulates Leptin Signal Transduction in Vivo. *Dev. Cell* **2002**, *2*, 489–495.
- For recent reviews on PTP1B inhibitors, see the following. (a) Burke, T. R., Jr.; Zhang, Z.-Y. Protein Tyrosine Phosphatases: Structure, Mechanism, and Inhibitor Discovery. *Biopolymers* **1998**, *47*, 225–241. (b) Moller, N. P. H.; Iversen, L. F.; Andersen, H. S.; McCormack, J. G. Protein Tyrosine Phosphatases (PTPs) as Drug Targets: Inhibitors of PTP1B for the Treatment of Diabetes. *Curr. Opin. Drug Discovery Dev.* **2000**, *3*, 527–540. (c) Blaskovich, M.; Kim, H.-O. Recent Discovery and Development of Protein Tyrosine Phosphatase Inhibitors. *Expert Opin. Ther. Pat.* **2002**, *12*, 871–905. (d) Johnson, T. O.; Ermolieff, J.; Jirousek, M. R. Protein Tyrosine Phosphatase 1B Inhibitors for Diabetes. *Nat. Rev. Drug Discovery* **2002**, *1*, 696–709.
- Robert, A. S. Isatoic Anhydride Derivatives. U.S. Patent 3,238,201, 1966.
- Scherrer, R. A.; Beatty, H. R. Preparation of *o*-Substituted Benzoic Acids by the Copper(II)-Catalyzed Reaction of Diphenyliodonium-2-Carboxylate with Anilines and Other Nucleophiles. *J. Org. Chem.* **1980**, *45*, 2127–2131.
- Shuker, S. B.; Hajduk, P. J.; Meadows, R. P.; Fesik, S. W. Discovering High-Affinity Ligands for Proteins: SAR by NMR. *Science* **1996**, *274*, 1531–1534.
- Hajduk, P. J.; Sheppard, G.; Nettlesheim, D. G.; Olejniczak, E. T.; Shuker, S. B.; Meadows, R. P.; Steinman, D. H.; Carrera, G. M.; Marcotte, P. A.; Severin, J.; Walter, K.; Smith, H.; Gubbins, E.; Simmer, R.; Holzman, T. F.; Morgan, D. W.; Davidsen, S. K.; Fesik, S. W. Discovery of Potent Nonpeptide Inhibitors of Stromelysin Using SAR by NMR. *J. Am. Chem. Soc.* **1997**, *119*, 5818–5827.
- Iversen, L. F.; Andersen, H. S.; Branner, S.; Mortensen, S. B.; Peters, G. H.; Norris, K.; Olsen, O. H.; Jeppesen, C. B.; Lundt, B. F.; Ripka, W.; Moller, K. B.; Moller, N. P. Structure-Based Design of a Low Molecular Weight, Nonphosphorus, Nonpeptide, and Highly Selective Inhibitor of Protein–Tyrosine Phosphatase 1B. *J. Biol. Chem.* **2000**, *275*, 10300–10307.
- Hajduk, P. J.; Augeri, D. J.; Mack, J.; Mendoza, R.; Yang, J.; Betz, S. F.; Fesik, S. W. NMR-Based Screening of Proteins Containing <sup>13</sup>C-Labeled Methyl Groups. *J. Am. Chem. Soc.* **2000**, *122*, 7898–7904.
- Refined crystallographic coordinates for the structure of PTP1B complexed with compounds **8b** and **17** have been deposited with the Protein Data Bank ([www.rcsb.org](http://www.rcsb.org)) with entry codes 10NZ and 10NY, respectively.
- Iversen, L. F.; Andersen, H. S.; Moller, K. B.; Olsen, O. H.; Peters, G. H.; Branner, S.; Mortensen, S. B.; Hansen, T. K.; Lau, J.; Ge, Y.; Holsworth, D. D.; Newman, M. J.; Moller, N. P. H. Steric Hindrance as a Basis for Structure-Based Design of

- Selective Inhibitors of Protein-Tyrosine Phosphatases. *Biochemistry* **2001**, *40*, 14812–14820 and references therein.
- (21) Glover, N. R.; Tracey, A. S. Nuclear Magnetic Resonance and Restrained Molecular Dynamics Studies of the Interaction of an Epidermal Growth Factor-Derived Peptide with Protein Tyrosine Phosphatase 1B. *Biochemistry* **1999**, *38*, 5256–5271.
- (22) Puius, Y. A.; Zhao, Y.; Sullivan, M.; Lawrence, D. S.; Almo, S. C.; Zhang, Z.-Y. Identification of a Second Aryl Phosphate-Binding Site in Protein-Tyrosine Phosphatase 1B: A Paradigm for Inhibitor Design. *Proc. Natl. Acad. Sci. U.S.A.* **1997**, *94*, 13420–13425.
- (23) Salmeen, A.; Andersen, J. N.; Myers, M. P.; Tonks, N. K.; Barford, D. Molecular Basis for the Dephosphorylation of the Activation Segment of the Insulin Receptor by Protein Tyrosine Phosphatase 1B. *Mol. Cell* **2000**, *6*, 1401–1412.
- (24) Burke, T. R.; Yao, Z.-J.; Liu, D.-G.; Voight, J.; Gao, Y. Phosphotyrosylmimetics in the Design of Peptide-Based Signal Transduction Inhibitors. *Biopolymers* **2001**, *60*, 32–44 and references therein.
- (25) Kay, L. E.; Keifer, P.; Saarinen, T. Pure Absorption Gradient Enhanced Heteronuclear Single Quantum Correlation Spectroscopy with Improved Sensitivity. *J. Am. Chem. Soc.* **1992**, *114*, 10663–10665.
- (26) Hajduk, P. J.; Gerfin, T.; Boehlen, J.-M.; Häberli, M.; Marek, D.; Fesik, S. W. High-Throughput Nuclear Magnetic Resonance-Based Screening. *J. Med. Chem.* **1999**, *42*, 2315–2317.
- (27) Lubben, T.; Clampit, J.; Stashko, M.; Trevillyan, J.; Jirousek, M. R. In *Current Protocols in Pharmacology*; Enna, S. J., Williams, M., Ferkany, J. W., Kenakin, T., Porsolt, R. D., Sullivan, J. P., Eds.; Wiley: New York, 2001; pp 3.8.1–3.8.18.
- (28) Liu, G.; Henry, K. J., Jr.; Szczepankiewicz, B. G.; Winn, M.; Kozmina, N. S.; Boyd, S. A.; Wasicak, J.; von Geldern, T. W.; Wu-Wong, J. R.; Chiou, W. J.; Dixon, D.; Opgenorth, T. J. Pyrrolidine-3-carboxylic Acids as Endothelin Antagonists. 3. Discovery of a Potent, 2-Nonaryl, Highly Selective ET<sub>A</sub> Antagonist (A-216546). *J. Med. Chem.* **1998**, *41*, 3261–3275.

JM0205696